RSC Advances

PAPER

View Article Online
View Journal | View Issue

Check for updates

Cite this: *RSC Adv.*, 2021, **11**, 23881

Increased sanitization potency of hydrogen peroxide with synergistic O_3 and intense pulsed light for non-woven polypropylene

Robin Jeong,[a] Hitendra Kumar,[ab] Steven Jones,[c] Allen Sandwell,[a] Keekyoung Kim[a] and Simon S. Park[*a]

Supplies of respiratory masks have recently become a concern due to the onset of the SARS-CoV-2 pandemic. Sanitization and reuse of masks can alleviate high mask consumption and production stresses. In the present work, improved sanitization potency of vaporous hydrogen peroxide (VHP) treatment of resilient bacterial spores while retaining polymeric filter performance was explored. A batch fumigation chamber with hydrogen peroxide (H_2O_2) vapor and ozone (O_3) is featured, followed by intense pulsed light (IPL) flash treatments. A resilient bacterial indicator, *Geobacillus stearothermophilus* (*G. stearothermophilus*), was utilized to compare the efficacy of various H_2O_2 concentrations in combination with O_3 and IPL. It was found that exposure to 30 minutes of 4.01 L min^{-1} 0.03% H_2O_2 aqueous vapor and 3 g h^{-1} O_3 followed by 10 IPL flashes per side completely inactivated *G. stearothermophilus*. The xenon sourced IPL irradiation was found to synergistically enhance radical production and strengthen the complementary biocidal interaction of H_2O_2 with O_3. Due to the synergistic effects, H_2O_2 was able to sanitize at a diluted concentration of 0.03% H_2O_2. The physical properties, such as surface potential, tensile strength, hydrophobicity, and filtration efficiency of >300 nm saline water aerosol of fibrous polypropylene (PP) sheets, were maintained. In addition, no residue of sanitizers was detected, thus confirming the biosafety and applicability of this method to disposable masks. Performance was benchmarked and compared with commercially available processes. The synergistic regime was found to achieve sterilization of *G. stearothermophilus* at drastically reduced H_2O_2 concentrations and in ambient conditions relative to commercial methods.

Received 11th May 2021
Accepted 30th June 2021

DOI: 10.1039/d1ra03675k

rsc.li/rsc-advances

Open Access Article. Published on 07 July 2021. Downloaded on 12/5/2025 4:10:48 AM.
This article is licensed under a Creative Commons Attribution-NonCommercial 3.0 Unported Licence.

1. Introduction

The coronavirus 2019 (COVID-19) pandemic caused by the severe acute respiratory syndrome coronavirus 2 (SARS-CoV-2) has resulted in a dramatic shift in everyday routine. Additional lawfully enforced measures such as travel restrictions, physical distancing, and mask-wearing guidelines have placed unique economic and societal stresses worldwide. Mask wearing has now become ubiquitous with normal life. These unprecedented measures are a necessary response to the over 98.2 million cumulative worldwide COVID-19 cases, of which around 3.2 million have died as of April 2021.[1] The World Health Organization (WHO) estimates that approximately 89 million medical-grade masks per month will be required to respond to the COVID-19 pandemic.[2] Due to the high demands for personal protective equipment (PPE) for high-risk persons (healthcare workers, elderly persons, persons with underlying health conditions), the public has been advised to utilize non-medical grade masks.

The PPE recommendation from various institutions emphasizes primarily wearing a face cover designed to cover the mouth and nose. Several types of masks and face-shields have been deployed for this purpose. High-risk persons require high efficiency PPEs such as N95 grade masks to protect from continuous exposure or due to increased vulnerability. These respirators help prevent exposure to droplets suspended in the air that may contain SARS-CoV-2 and thus require a fitting test to ensure tight sealing. Furthermore, these cannot be conventionally washed, which limits their disinfection avenues. To conserve higher grade PPEs, surgical or loose-fitting disposable masks have been recommended to the public as these can be more easily fabricated. Popular materials for fabricating these masks also include cotton, silk, chitosan, and polypropylene (PP). A recent study evaluated the efficacy of various cotton-based masks and found cotton-silk as one of the more effective fabric combinations.[3] However, both N95 respirators and

[a]*Department of Mechanical and Manufacturing Engineering, University of Calgary, Calgary, Alberta T2N 1N4, Canada. E-mail: simon.park@ucalgary.ca; Tel: +1 403 220 6959*

[b]*School of Engineering, The University of British Columbia, Kelowna, BC V1V 1V7, Canada*

[c]*Zymetrix Biomaterials & Tissue Engineering Technology Development Centre, Calgary, Alberta T2N 1N4, Canada*

© 2021 The Author(s). Published by the Royal Society of Chemistry

Open Access Article. Published on 07 July 2021. Downloaded on 12/5/2025 4:10:48 AM.
This article is licensed under a Creative Commons Attribution-NonCommercial 3.0 Unported Licence.

surgical masks are often fabricated using PP fibers. These PP based non-woven masks are suitable for mass production while retaining breathing comfortability due to a less dense (thinner) filter piece.

Sanitization and reuse of PPEs such as facepiece respirators are possible and outlined by various studies.[4–8] This would also minimize contaminated wastes designated for landfills. Filtration efficiency of polymeric masks is reliant on various mechanisms including electrostatic capture.[6] Electrostatically dependent or electret filters can achieve filtration of smaller particles while minimizing fiber density. Electrostatic properties on PP based masks are necessary to effectively capture sub-300 nm droplets or even possibly the virus itself which has a mean size around 100 nm.[9] Therefore, sanitization methods for polymeric masks must preserve or regenerate the electrostatic potential while maintaining structural integrity. Three methods of sanitization are recommended by the Center for Disease Control (CDC): vaporous hydrogen peroxide (H_2O_2) (VHP) treatment, ultraviolet germicidal irradiation (UGI), and moist heat treatment at 60 °C. These methods have shown at least 99.99% antimicrobial efficacy against contaminants such as *Geobacillus stearothermophilus* (*G. stearothermophilus*) spores, Influenza A (H1N1), SARS-CoV, and Avian influenza A virus (H5N1). These treatment methods have also produced sanitized N95 grade filters with acceptable filtration efficiency post sanitization. Other high temperature-based sterilization methods, such as microwave or autoclaves, are not recommended as they can melt PP fibers. The use of alcohol is also not recommended as alcohol treatment can strip electrostatic charge properties from electret-based filters.

However, the CDC advises the public not to sanitize and reuse loose-fitting disposable masks. Most disposable masks are not intended for reuse as they cannot be deemed safe nor reliably resistant to sanitization methods. Household sanitization methods, such as soaking and washing, have previously shown a severe loss in filtration efficiency despite no physical damage to the fibers.[6] Therefore, contactless treatments, such as UGI or heat, are recommended but require a lengthy treatment cycle.[6]

UGI appropriate lamps are widely available for off-the-shelf use; however, the UGI processes can be lengthy and easily obstructed. Heated sanitization methods that require controlling humidity levels and steam treatment has been proven to inoculate various viruses, including the SARS-CoV-2.[10] For example, simple disinfection *via* microwave generated steam is available in most households. However, continuous steam treatment runs the risk of degenerating a masks surface charge. Ou *et al.*[6] and Pirker *et al.*[11] found filtration efficiency losses in electret-based masks after 5 to 10 cycles of steam exposure for 30 min, which was attributed to the condensation of water droplets that can strip surface charge. Furthermore, Ou *et al.*[6] observed an unacceptable loss in filtration efficiency in surgical and procedure masks after being immersed in isopropyl alcohol (IPA).[6] A shift in the most-penetrating particle size (MPPS) to a much larger size range after IPA immersion indicated a loss in electrostatic charge-based action, which is a typical observation when alcohol and soap-based sanitization methods are used. The group found acceptable filtration performance from masks that were sanitized by VHP, UGI, and thermal methods. However, certain limitations exist in industrial-scale sanitization. UGI treatment has limited throughput due to the required surface area exposure to lamp irradiation. Moist heat treatment requires precise control of humidity to avoid long treatment times.[6] H_2O_2 vapour treatment requires consumption of H_2O_2 as well as possible toxic residues left on the mask. In addition, quantitative direct surface electrostatic charge observations before and after treatment of non-medical masks and their correlation to filter efficacy are lacking.

The efficacy of H_2O_2 can be further improved by introducing a UV irradiation source that can provide the necessary energy to drive the breakdown of the H_2O_2 molecules into biocidal reactive oxygen species (ROS). This method is commonly referred to as an advanced oxidation process and is typically used for wastewater treatment in which free radicals attack and mineralize contaminants such as sewage or pharmaceutical waste.[12] Alkawareek *et al.*[13] utilized a composition of H_2O_2 and silver nanoparticles (AgNPs) with strong antibacterial effects at a concentration 100 times lower than the commonly used 3–6% for disinfecting surfaces. They attributed the increased antibacterial efficacy to a Fenton-like synergistic effect of H_2O_2 with AgNPs. *Escherichia coli* and *Staphylococcus aureus* were used as model organisms with exposure to H_2O_2 and AgNPs in a liquid medium. This significantly improved sterilization; however, its application was mostly focused towards hard surface disinfection.[13] Antibacterial effects of H_2O_2 were also studied in recent works by using *G. stearothermophilus* as a model organism. It was demonstrated that H_2O_2 fogging was able to kill the spores; however, longer contact times ranging from 60 minutes to 200 minutes and higher concentration of H_2O_2 ranging from 5% to 35% were required.[14,15] These conditions highlight the need for an efficient H_2O_2 based sterilization approach to reduce both processing time and the concentration of H_2O_2.[15]

In response to the above challenges, we aimed to develop a novel sanitization method that increases the potency of VHP while retaining filter performance after treatment. PP based filter sheets was selected as the mask analogue. A simulated contaminant in the form of *G. stearothermophilus* was used to assess the biocidal potency. In addition, PP filter sheets can simulate potential changes in PP based masks after exposure to various sanitization regimes. We chose *G. stearothermophilus* due to its extremophile classification, making it hard to sterilize thus resulting in its widespread use for sanitization benchmarking.[16] The goal is to produce an optimized sanitization condition that increases the potency of H_2O_2 during VHP treatment while ensuring safe reuse of sanitized filters. Synergistic elements O_3, and IPL were introduced to improve the potency of VHP sanitization. This novel combination was explored at decreasing aqueous H_2O_2 concentrations. Sanitization efficacy and biosafety was evaluated by 24 hour incubation of treated spore discs and FT-IR analysis of PP sheets, respectively. Retention of PP filtration efficiency was evaluated with filtration tests of >300 nm saline droplets and electrostatic surface potential measurements before and after sanitization. In addition, mechanical strength of the PP sheets before and

© 2021 The Author(s). Published by the Royal Society of Chemistry

Open Access Article. Published on 07 July 2021. Downloaded on 12/5/2025 4:10:48 AM.
This article is licensed under a Creative Commons Attribution-NonCommercial 3.0 Unported Licence.

after treatment was quantified *via* tensile testing. By introducing synergistic elements O_3 and IPL, biocidal potency was improved; this facilitates lower H_2O_2 consumption which allows scaling to larger operations or augmenting existing methods to reduce the sanitization time.

2. Experimental

2.1 Sanitization experimental setup

G. stearothermophilus spore discs were subjected to various sanitization processes to optimize the synergetic biocidal effect of H_2O_2, O_3, and IPL. Glass fiber discs (9 mm in diameter) laden with *G. stearothermophilus* spores (2.1×10^6 cells per disc) were used for this purpose (GFTS-6, Crosstex, Hauppauge, NY, USA). Fumigation and IPL treatment of indicator spores and PP sheets were performed in a custom 13.4 L capacity acrylic cylindrical chamber (24.5 cm in diameter and 28.5 cm in height), as shown in Fig. 1. The chamber features two perpendicular inlets for O_3 and H_2O_2 vapour with an outlet to a condenser (Fig. 1). The H_2O_2 vapour and O_3 were generated *via* a single jet 6.89 kPa collision nebulizer (CN241 Collision 1-Jet MRE type, BGI Inc, Waltham, MA, USA) and a 3 g h^{-1} O_3 generator, respectively. To observe the limits of sanitization efficacy with and without synergistic elements, 3% v/v H_2O_2 was diluted to lower volume concentrations with distilled water prior to being fed to the nebulizer. Individual flow controllers (Omega FMA5520A, Omega Engineering, Norwalk, CT, USA) were used to maintain and measure the H_2O_2 and O_3 flows. The H_2O_2 flow was controlled at 4.01 L min^{-1} while O_3 was allowed to flow freely. The O_3 flow was measured at 5.50 L min^{-1} thus assuming performance at the rated 3 g h^{-1} indicates about 0.42% of the flow is O_3 by volume. The chamber was enclosed with a removable 32 mm thick glass cover, which supported a 4800 W s xenon flash lamp (Speedotron model 4803, Speedotron, Chicago, IL, USA) with a 6 ms irradiation pulse. The xenon flash lamp provided a broadband light source, characterized in a previous study, with wavelengths between 300 to 900 nm.[17]

2.2 Sanitization exposure and spore incubation

The *G. stearothermophilus*-laden fiberglass spore discs and 0.4 mm thick PP filter sheets were treated with various

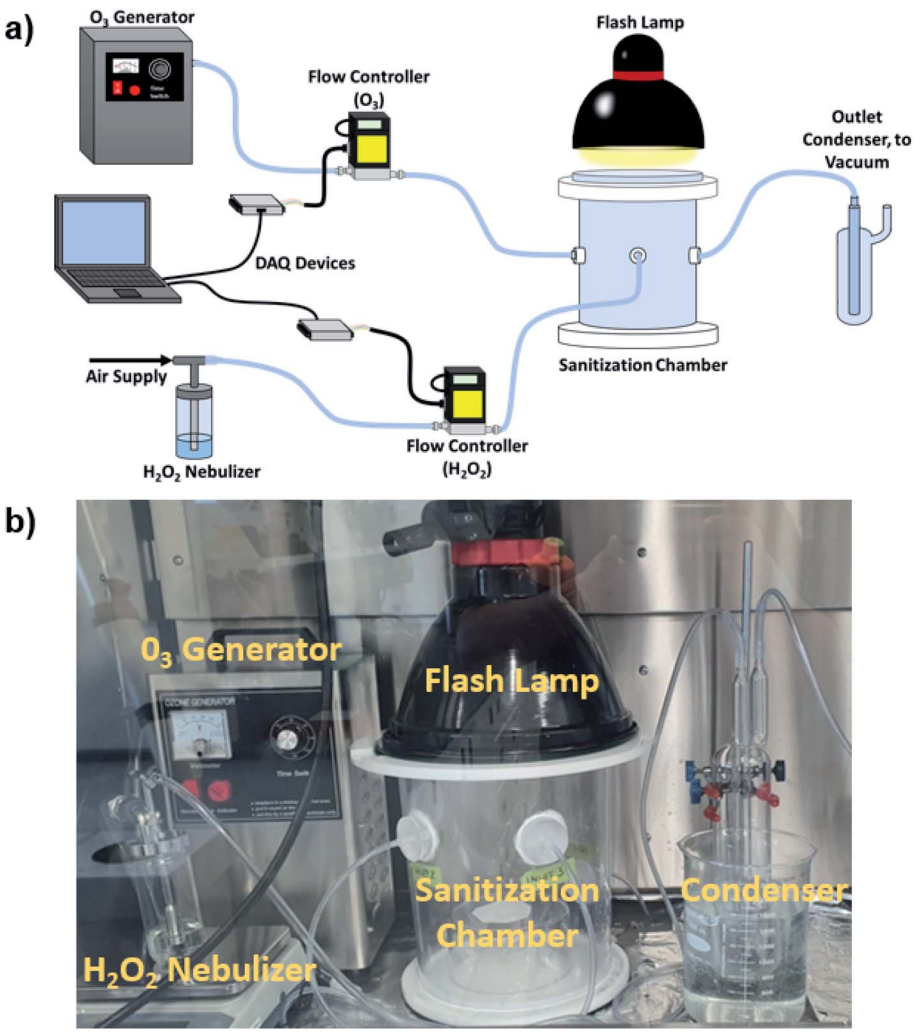

Fig. 1 (a) Sanitization chamber schematic. (b) Experimental setup.

Open Access Article. Published on 07 July 2021. Downloaded on 12/5/2025 4:10:48 AM.
This article is licensed under a Creative Commons Attribution-NonCommercial 3.0 Unported Licence.

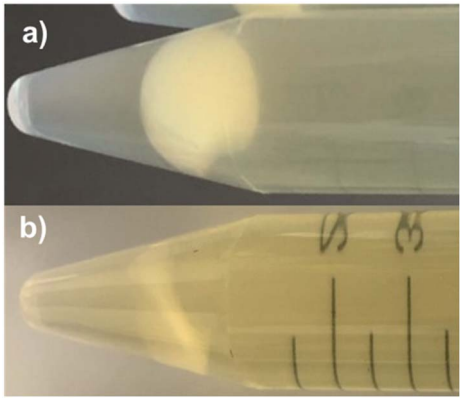

Fig. 2 (a) Broth with surviving spores (1% H_2O_2 fumigation) is evident by turbidity compared to (b) thoroughly sanitized and clear broth (0.05% H_2O_2 + O_3 + flash) after 24 h incubation. Note the visibility of the test tube's graduation. All, including the pictured samples, were fumigated for 30 min followed by 10 flashes per side where applicable.

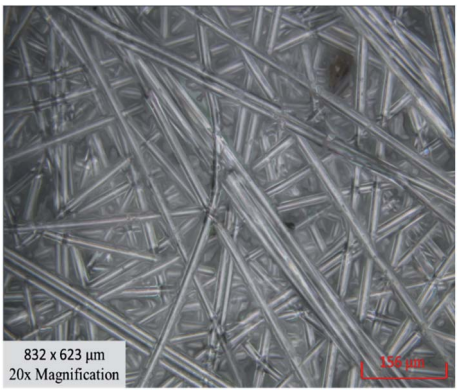

Fig. 3 Optical profilometer (Zeta-20, KLA, Milpitas, CA, USA) image of PP sheets under 20× magnification utilized for physical integrity, surface residue, surface potential, and filtration efficiency experimentations. A mean fiber diameter of 15 µm was observed.

combinations of H_2O_2 vapour and O_3 with and without post-fumigation IPL. The samples were suspended in-level with the inlet flows and maintained in the chamber for 30 minutes of fumigation. Once fumigated, the chamber was evacuated, and the samples were placed 20 cm below the xenon lamp for IPL exposure. All the samples were handled with sterilized steel tweezers and placed with their radial faces perpendicular to the flashlight, irradiated, and then flipped for exposure on both sides. After the *G. stearothermophilus* spore-laden discs were exposed to various sanitization conditions, the spores were incubated to expose any surviving bacterium. The spore samples were immersed in tryptic soy broth (TSB) and incubated at 37 °C for 24 hours. Incomplete inactivation of spores was evident from a visible increase in turbidity of the TSB after incubation. Successful or total inactivation of spores after treatment was evident from the retention of TSB clarity after 24 hour incubation (Fig. 2).

2.3 Physical characterizations

After identifying the optimal sanitization regime that utilizes the minimum amount of H_2O_2, the effect of this optimized condition on PP filter sheets is examined. PP filter sheet's tensile strength, surface residue, and surface potential was examined before and after exposure to the sanitization processes. The physical integrity of the PP samples was examined by performing tensile tests (ESM303, Mark-10, Copiague, NY, USA). 100 mm × 15 mm rectangular PP sheet samples with average fiber diameters of 15 µm (Fig. 3) were mounted on the Mark-10 tensile tester and subjected to a strain rate of 15.0 mm min^{-1}. As all sheet samples were prepared with the same cross-sectional dimensions, earlier (strain value) or lower yield stress was regarded as evidence of mechanical degradation.

For surface residue and surface potential experiments, 1 cm × 3 cm PP sheets were cut and used. Attenuated total reflection (ATR) FT-IR analysis was performed to identify any sanitizer residue left after treatment. To observe changes in surface potential due to the sanitization treatment, a non-contact digital static field meter (DESCO 19492, DESCO, Chino, CA, USA) was used to measure the static surface potential of the PP sheets.

2.4 Filtration efficiency test

The filtration efficiency of the PP samples before and after sanitization treatment was evaluated using 300 nm to 3000 nm saline water aerosol. As shown in Fig. 4, the air from the laboratory compressed air supply was passed through a regulator set to 138 kPa. This regulator was used to feed both the ionizer (SMC IZN10, SMC Corporation, Tokyo, Japan) and nebulizer. The aerosol generated by the nebulizer was passed through a desiccant dryer before being introduced into the mixing chamber. To provide the required air volume for the particle counter (Kanomax 3905, Kanomax USA, Andover, NJ, USA), an additional regulator was used to supply air to the mixing chamber in combination with the air supplied by the ionizer and nebulizer. This supply line was also connected to open air to balance the inward and outward airflow in the mixing chamber. Solenoid valves were used to maintain consistent sampling of air from upstream and downstream of the test sample.

These experimental characterizations evaluated the limits of biocidal efficacy for the synergistic VHP process. By introducing O_3 and IPL, sanitization of *G. stearothermophilus* spore discs at diluted H_2O_2 concentrations can be achieved. Mask integrity tests were used to infer conservation of filtration efficacy and mechanical strength after exposure to the process. Retention of biosafety and filtration of smaller particles was examined by utilizing ATR FT-IR and surface potential characterizations, respectively.

3. Results

3.1 Sanitization with various conditions

Vaporous 3% H_2O_2 aqueous solution was unable to sanitize the spore discs after 30 min of 4.01 L min^{-1} fumigation while 24 h full immersion in aqueous 3% H_2O_2 was able to fully

© 2021 The Author(s). Published by the Royal Society of Chemistry

Open Access Article. Published on 07 July 2021. Downloaded on 12/5/2025 4:10:48 AM.
This article is licensed under a Creative Commons Attribution-NonCommercial 3.0 Unported Licence.

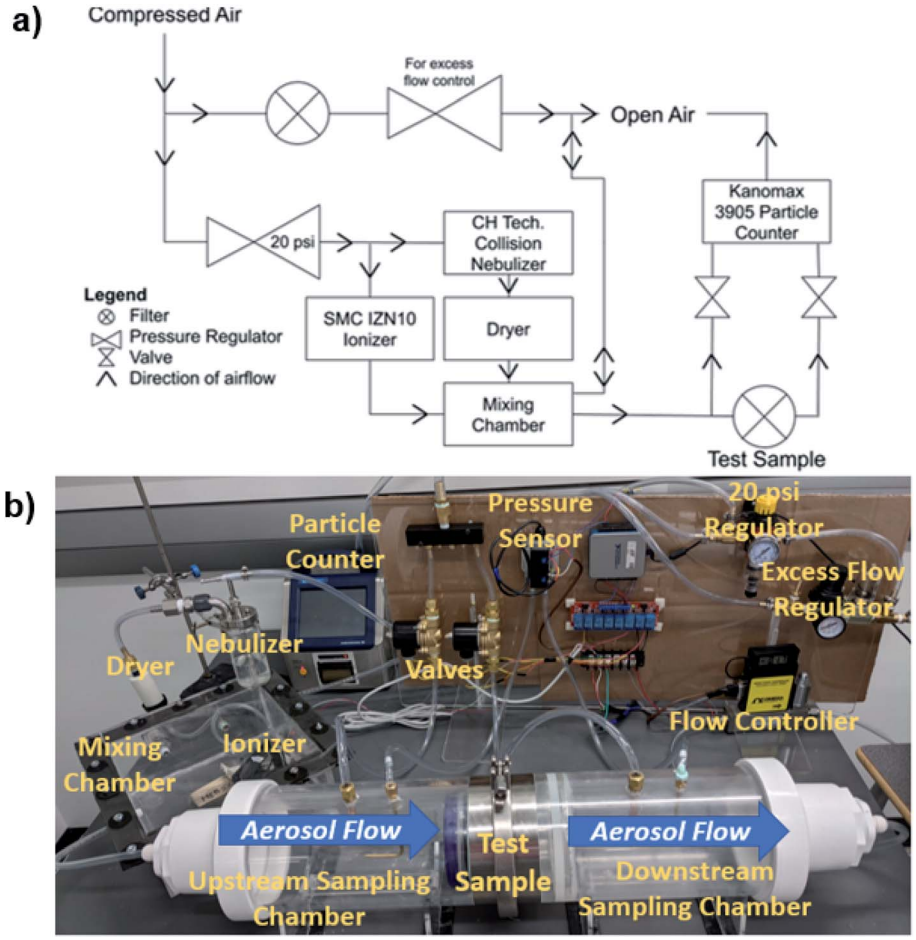

Fig. 4 (a) Filtration test schematic and (b) laboratory setup for filtration efficiency of aerosol saline water testing.

sanitize spore discs. However, full immersion or washing of polymeric filters is not advised as it can deteriorate the surface potential. Loss of surface potential will reduce the filtration efficiency of smaller particles. The mechanism in which washing the electret filters causes surface potential loss is further explored in Section 4.2. Additionally, the present O_3 generator rated at 3 g h^{-1} was unable to sanitize the spore discs on it own after 30 min fumigation. This lack of biocidal performance is attributed to the high stability of gaseous O_3 and insufficient exposure time or the lack of humidity control. Furthermore, IPL exposure alone (10 flashes per side) was unable to sanitize the spore discs. The poor performance of the IPL treatment is attributed to the emission spectrum from the xenon light source that was characterized in a previous study.[17] The present xenon flash lamp lacks emission components in the strongest UV light biocidal range of 100–280 nm, known as the UVC range. UVC irradiation, when absorbed by cells or microbe's DNA or RNA, induces damage or mutation mediated by the generation of free radical species. Consequently, this affects the microorganism's ability to replicate.[18] The present IPL source lacks a significant amount of the UVC component and is too brief to provide sufficient sanitizing action on the resilient spores on its own.

Various synergistic combinations of H_2O_2, O_3, and IPL flash sanitization results are shown in Table 1. Introducing IPL post-H_2O_2 fumigation yielded spore disc sterilization at H_2O_2 concentrations as low as 0.1%. The combination of 3% H_2O_2 and O_3 provided a strong sanitization action in contrast to these sanitizers' individual performances. The combination of H_2O_2, O_3, and IPL irradiation produced a further improved synergistic effect. This H_2O_2/O_3/IPL combinate achieved sterilization of *G. stearothermophilus* with an H_2O_2 aqueous vapour concentration as low as 0.03%.

Thus, the synergetic effect of H_2O_2, O_3, and IPL was optimized to sterilize *G. stearothermophilus* at a severely reduced H_2O_2 concentration. This resulted in an optimal sanitization condition of 0.03% H_2O_2 vapor at 4.01 L min^{-1} and 3 g h^{-1} O_3 exposure for 30 minutes, followed by ten flashes per spore disc face (Table 1). The optimized condition lowered the consumption of H_2O_2 about 3-fold relative to using 0.1% H_2O_2 + IPL by introduction of O_3 while retaining a sanitization potency capable of eliminating *G. stearothermophilus* spores. For reference, the commercially available Bioquell BQ-50 is able to achieve total sterilization of *G. stearothermophilus* after 20 min of VHP treatment with 35% H_2O_2.[15] Assuming the maximum setting for inlet flow of 16 g min^{-1} H_2O_2 for the BQ-50, the

Open Access Article. Published on 07 July 2021. Downloaded on 12/5/2025 4:10:48 AM.
This article is licensed under a Creative Commons Attribution-NonCommercial 3.0 Unported Licence.

Table 1 Synergetic performance of various sanitization conditions

Testing	H_2O_2 (% volume)	O_3 (g h^{-1})	Flash number (per side)	Result
H_2O_2 + IPL	3.00%		10	Sanitized
	2.00%			
	1.00%			
	0.30%			
	0.20%			
	0.10%			
	0.03%			Incubated
	0.01%			
H_2O_2 + O_3	3.00%	3		Sanitized
Synergetic H_2O_2 + IPL + O_3	0.05%	3	10	Sanitized
	0.03%			

optimized synergistic condition presents a 67.8% decrease in H_2O_2 consumption. Although not present in Table 1, the reduction of flash number was investigated. However, flash pulses lower than 10 per side resulted in incubation with 3% H_2O_2 and O_3. Thus, 10 flash pulses (6 ms) per side was kept standard in this study. The optimal sanitization condition of 4.01 L min^{-1} of 0.03% H_2O_2 vapor and 3 g h^{-1} O_3 exposure for 30 minutes followed by ten flashes per substrate/sheet side will be referred to as the optimized condition/regime.

3.2 Filtration efficiency and surface potential

It is important to note that the saline droplet filtration test was performed to confirm the absence of significant mechanical damage and loss in filtration efficiency of larger particles (>300 nm). Surface potential changes would incur a severe loss in filtration efficiency of particle sizes below the 300 nm range, which the present particle counter cannot detect.[6,11,19] Degeneration of the mechanical integrity of PP has not been observed in most vaporous hydrogen peroxide experiments.[20,21] PP has generally been considered compatible with H_2O_2, and serious mechanical degeneration of PP is only a concern with high heat or intense mechanical washing. Due to the heat generated from the IPL xenon-lamp, the masks must be evaluated for thermal damage. Triplicate experiments revealed PP sheets retained the filtration efficiency of 300 nm to 3000 nm saline droplets after exposure to the optimized regime with deviations within measurement error (Fig. 5a).

Polypropylene ranks relatively negative in the triboelectric series and is likely to interact strongly with aqueous H_2O_2. This phenomenon was confirmed by comparing surface charge measurements before and after full immersion of PP sheets in 3% aqueous H_2O_2 of PP sheets. The PP samples soaked in 3% H_2O_2 followed by 12 h of drying exhibited 74% decrease in surface potential magnitude (Fig. 5b). This contrasted with the 1.6% and 5% surface potential change on PP sheets treated with 30 min of 0.03% H_2O_2 vapour and the optimized 0.03% H_2O_2 vapor + O_3 + IPL condition, respectively. At a constant pressure and temperature, the dew point of a vaporous mixture of water and H_2O_2 is dependent on H_2O_2 concentration. At an increasing concentration of H_2O_2, the maximum water vapour saturation pressure will decrease and will facilitate condensation. By utilizing a dilute 0.03% aqueous H_2O_2 vapours, potential condensation was minimized.

It should be noted that certain systems utilize condensation to improve the decontamination performance of vaporous H_2O_2. However, the biocidal enhancement of condensed H_2O_2 is still debated and certain studies even suggest a dry

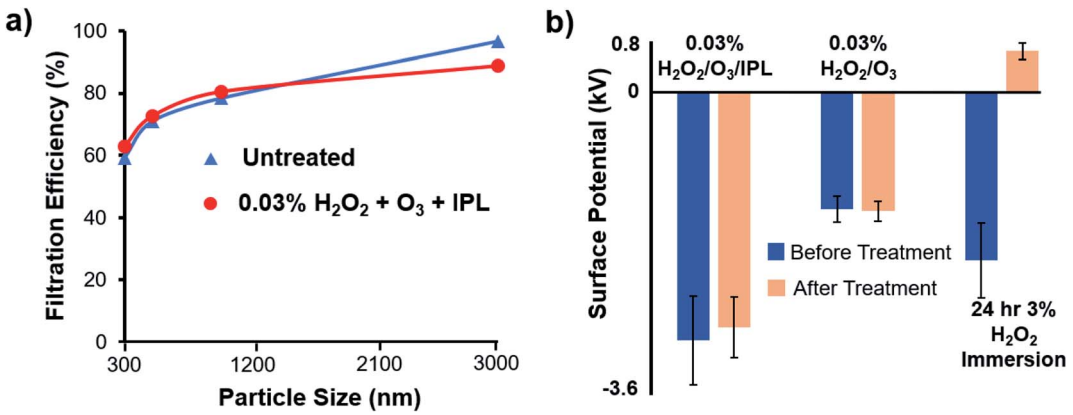

Fig. 5 (a) Filtration efficiency of PP sheets before and after exposure to the optimized condition. (b) Change in surface potential of PP sheets after exposure to various sanitization conditions.

© 2021 The Author(s). Published by the Royal Society of Chemistry

Open Access Article. Published on 07 July 2021. Downloaded on 12/5/2025 4:10:48 AM.
This article is licensed under a Creative Commons Attribution-NonCommercial 3.0 Unported Licence.

environment facilitates greater H_2O_2 biocidal action.[22,23] It should also be noted that the static field meter used for surface potential measurements only provide a potential value proportional to the actual surface potential. However, the static field meter is still able to capture the polarity and relative magnitude changes in electrostatic potential of PP sample surfaces. Furthermore, despite precautions during handling, the initial magnitude of the sheets differs due to changes in surface potential during storage. In addition to taking precaution during handling to minimize affecting the surface potential, all experiments were performed in triplicate and sourced from the same roll of PP filter sheet.

3.3 Tensile strength and biosafety

Tensile strength tests were performed to examine any losses in mechanical strength after sanitization (Fig. 6a). Triplicate tests found yield stresses of 1.75 ± 0.17 and 1.70 ± 0.25 MPa for optimized condition treated and untreated PP sheets, respectively; these values were observed at 3.03% and 3.97% strain for optimized condition treated and untreated PP sheets, respectively. The treated PP sample showed slight embrittlement evidenced by an increase of the modulus of elasticity compared to the non-treated PP sample. It should be noted that after the yield stress, significant tearing was observed. The strain region past the yield point was considered as a total failure of the PP sheet integrity. H_2O_2 overall is required to be present at relatively high concentrations as well as in heated environments to cause any serious decay in PP integrity by oxidative processes.[24] This is also found to be true for both excessive O_3 and UV-light exposure.[11,25,26] However, the proposed room temperature sanitization method minimized physical damage to the PP fibers.

To confirm the removal of any residual sanitizers, FT-IR spectra of non-woven PP sheets before and after sanitization were analyzed for the presence of H_2O_2 and O_3 species. The optimized sanitization condition of 0.03% H_2O_2 vapour exposure and 3 g h^{-1} O_3 fumigation for 30 min was performed on PP sheets, with and without IPL irradiation. As shown in Fig. 6b, none of the PP sheet samples provided detectable amounts of H_2O_2 and O_3 in their ATR FT-IR spectra, performed in triplicate. The control untreated PP sheet exhibited strong peaks in the 3000–2800 cm^{-1} range attributed to CH_3 asymmetric and symmetric vibrations. In addition, distinct 1460 cm^{-1} and 1378 cm^{-1} peaks associated with CH_3 asymmetric and symmetric deformations were also present.[27] When normalized based on the PP control spectrum, neither bands or peaks associated with H_2O_2 and O_3 were observed in any of the samples, including fully immersed and direct sprayed. This was further corroborated by the lack of any 3200–3150 cm^{-1} bands representing O–H bonds. In addition, the near identical spectra suggest little change in the chemical structure of the PP sheets. This was also indicated by an only minor embrittlement observed during tensile tests after exposure to the optimized sanitization regime. This can be the result of the relatively short lifetime of H_2O_2 and O_3 on surfaces before they decompose to benign products such as water and oxygen.[22,23] PP has also been reported to have limited interactions and good chemical compatibility with present sanitizers. This was especially evident in ambient temperatures and short exposure times.[25,28]

The lack of interaction between the PP sheets and present aqueous sanitizers is further reduced by the high hydrophobicity of PP. To verify the minimal chemical and physical effects of the optimized regime, contact angle measurements were taken with distilled water droplets. Retention of hydrophobicity in PP sheets was observed by measuring their contact angles with static water droplets prior to and post sanitization. The initial contact angle was measured to be 146° while the contact angle post sanitization was measured to be 133°. This small decrease in the contact angle suggested that there may be a slight increase in the wetting effect but the overall hydrophobicity of the PP sheets was retained.

4. Discussions

4.1 Individual and synergistic sanitization mechanisms

H_2O_2 is utilized extensively for antimicrobial and antiviral applications, including disinfection of surfaces and porous materials. Often used in the form of an >3% aqueous solution or >30% vapors, the biocidal properties of H_2O_2 arise from its

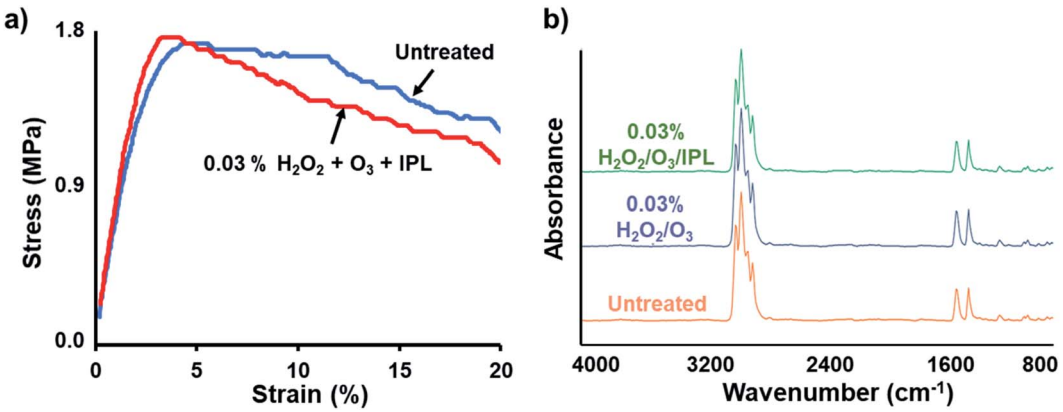

Fig. 6 (a) Tensile strength of PP sheets untreated and treated with optimized condition. (b) ATR FT-IR spectra of PP sheets at various conditions and treatment. Fumigation was performed for 30 min and IPL flashes applied 10 times per side where applicable.

Open Access Article. Published on 07 July 2021. Downloaded on 12/5/2025 4:10:48 AM.
This article is licensed under a Creative Commons Attribution-NonCommercial 3.0 Unported Licence.

oxidizing nature due to the generation of the ROS which include superoxide (O_2^{*-}) and hydroxide (OH*) radicals (Fig. 7).[29] The hydroxyl radicals can also be generated by the Fenton reaction. In the Fenton reaction, Fe^{2+} in the presence of H_2O_2 catalyzes the reaction to generate hydroxyl radicals (Fe^{2+} being present in various amounts in cells bound to DNA). Previous studies have also suggested a time-dependent biocidal action of H_2O_2 within cells comprising of two modes. In the first mode, a low concentration of H_2O_2 results in DNA damage to kill the cells. In the second mode, a high concentration of H_2O_2 results in cell death by targeting other organelles. Within the cells, H_2O_2 oxidizes several amino acid residues independent of the presence of metal ions. This causes modifications of the protein side groups or, in some cases, complete cleavage of the protein backbone, leading to cell death. The ROS generated from H_2O_2 also lead to cell membrane and cell lipids damage. Furthermore, Brandi *et al.*[30] found loss of cellular material was the cause of cell death when the bacteria cultures were treated with H_2O_2, indicating that H_2O_2 disrupts the cell membrane.

O_3 exhibits oxidative properties, which has attracted its use for antibacterial applications. O_3, often generated by a corona discharge device or UV light, is relatively stable in the gaseous phase mixed with oxygen or air. By simply sourcing ambient air, O_3 has the potential to be a readily available sanitizer that can easily penetrate porous structures.[31–33] Typically, O_3 is not considered an effective sanitizer below 50% relative humidity.[32] When dissolved in water, O_3 decays to form biocidal hydroxyl radicals (Fig. 7). Alone in the gaseous phase, O_3 is hypothesized to damage the cell membrane by reacting with: proteins, respiratory enzymes, unsaturated fatty acids, peptidoglycans, nucleic acids, spore coats, and virus capsids.[34] Thus, the present sanitization chamber with no environmental humidity control did not effectively utilize O_3 as a sanitizer with 30 min of exposure.

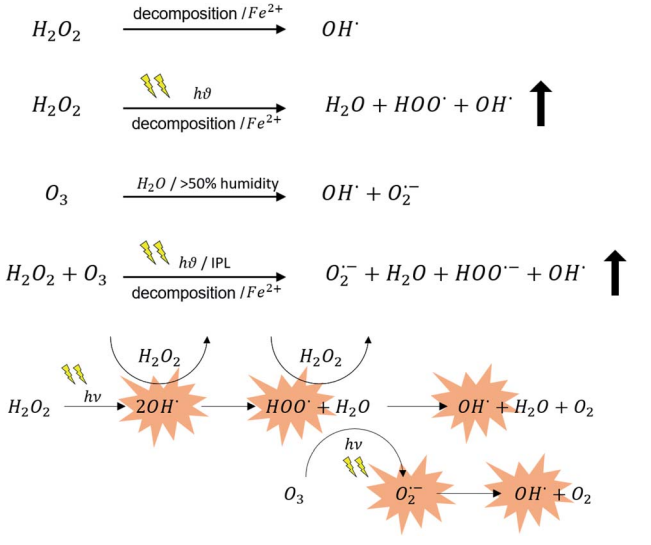

Fig. 7 Mechanisms for increased radical species during VHP treatment with the introduction of O_3 and IPL irradiation. ↑ indicates increased and rapid generation of OH* species. Species with red background are ROS and contribute to disinfection action.[29,30]

Previous studies found the requirement of H_2O_2 concentration in the presence of visible light to be several folds lower than the minimum inhibitory concentration of H_2O_2 for various bacteria strains.[35] It was also demonstrated that the mechanism of action did not involve the generation of more hydroxyl radicals but involved an 'activation' of H_2O_2 through light exposure. Physiological changes in the bacteria cells resulting from visible light exposure can also increase the vulnerability to lower concentrations of H_2O_2. Additionally, the photo-Fenton reaction was attributed to the improvement of the biocidal performance of H_2O_2 in the presence of light. The H_2O_2 interaction with intracellular Fe^{2+} is enhanced under blue light exposure, leading to irrecoverable damage of several proteins, nucleic acids, and various organelles.[35] This was attributed to advanced oxidation and the peroxide process, which enhances the production of reactive hydroxyl radicals and trioxidane (H_2O_3), a potent biocidal agent.[8,36]

Photolytic mechanisms of H_2O_3 production in the presence of H_2O_2 and O_3 were previously studied by isolation in argon matrices. Further analysis of H_2O_3 production in a peroxide system by Xu *et al.*[37] indicates an initial [(HOO)(HOOO)-7r] complex formation. In the presence of irradiation such as IPL, [(HOO)(HOOO)-7r] produces [(HOO)(HO)] complex which rapidly close to form H_2O_3. As stated earlier, H_2O_2 showed synergistic behavior with blue light exposure to result in a higher biocidal efficacy. The advanced oxidation process involving a combination of H_2O_2, O_3, and light exposure, however, has not been studied in-depth in the context of sanitization. A few studies, however, have used a H_2O_2/O_3/UV exposure system for chemical oxidation of municipal landfill leachate and oxidation of organic compounds.[38,39] When UV exposure was introduced, the decomposition of O_3 was accelerated, and H_2O_2 was formed as an intermediate species. In parallel, H_2O_2 decomposed and produced hydroxyl radical species, which were further activated by light exposure. Both reactions occurred simultaneously in the advanced oxidation process using a O_3/H_2O_2/light exposure system. The presence of H_2O_2 drove the UV-assisted O_3 decay process, resulting in a higher and more rapid yield of hydroxyl radical species. These species, in turn, exhibited biocidal characteristics. It was evident from these investigations that the advanced oxidation processes involving O_3/UV exposure and H_2O_2/light exposure enhances biocidal activity.

4.2 Filtration mechanism and physical properties

The filtration mechanism of various fibrous polymeric filters utilizes electrostatic forces. The fibers on these filters hold an electrostatic charge which allows them to capture particles smaller than the filter pore size (typically sub-300 nm). This allows for effective but relatively thin filters that can retain user comfort and breathability.[11,19] Previous studies have reported significant losses in filtration efficiency attributed to a loss in surface charge while visible mechanical damage was not present.[6] Loss in electrostatic charge during vaporous treatment or liquid washing can be attributed to the triboelectric effect. When water or sanitizer

© 2021 The Author(s). Published by the Royal Society of Chemistry

Open Access Article. Published on 07 July 2021. Downloaded on 12/5/2025 4:10:48 AM.
This article is licensed under a Creative Commons Attribution-NonCommercial 3.0 Unported Licence.

droplets condense, they carry and eventually remove a large magnitude of surface charge (see Fig. 8).

Although PP fiber density is kept at a minimum by utilizing electrostatic mechanisms, fiber density is still crucial in capturing larger particles or droplets. Mechanical degradation compromises both the filtration efficiency and resistance against stresses from regular handling and wear. The present sanitizing agents can damage the mechanical integrity of PP in a variety of ways. High concentration of O_3 has been found to attack and degrade the polymeric backbone of PP.[26] Brief exposure of H_2O_2 at diluted concentrations can minimize the rate of oxidative attack on PP. In addition, IPL exposure specifically in the biocidal UVC range has been found to have little affect on the mechanical properties of PP.[11] However, PP is susceptible to damage from heat which the broadband flashes do provide. Although brief, the introduction of heat can not only thermally damage PP but catalyze and intensify the oxidative attack of H_2O_2 on PP.[24] For the reuse of polymeric-based masks using the presented novel sanitization process, the filters must also be biosafe. Although H_2O_2 readily decomposes to become H_2O and O_2, prolonged H_2O_2 vapour inhalation can cause coughing and shortness of breath. O_3 is used for various medical applications; however, chronic exposure and inhalation can cause inflammation and shortness of breath.[41,42] Both O_3 and H_2O_2 have been found to cause skin irritations and skin damage at various levels based on the individual's sensitivity.

4.3 Current limitations and future prospects

The optimised sanitization condition of 30 min exposure of 4.01 L min^{-1} 0.03% H_2O_2 and 3 g h^{-1} O_3 followed by 10 IPL flashes per side was able to fully sterilize *G. stearothermophilus* spore discs. All aspects crucial to polymeric filter performance such as: electrostatic charge, biosafety, mechanical strength, hydrophobicity, and filtration efficiency were retained. It must be noted that although the optimized sanitization regime was successful on PP filter sheets, a different interaction may occur on other mask components such as disposable mask ear loops and metallic or plastic nose clips. Previous studies have found degeneration of ear loops' wearability after 20 to 50 cycles of sanitization.[20,21,43] However, the present H_2O_2 concentration is not only reduced by 67.7% relative to commercial products[15] but processed at ambient conditions for a short duration. These conditions are not expected to cause significant damage to other mask components.

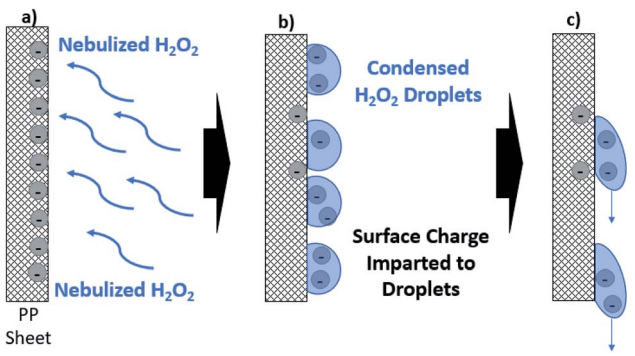

Fig. 8 Theorized mechanism of surface charge loss *via* condensed droplets. (a) PP sheet is exposed to H_2O_2 flow. (b) H_2O_2 droplets condense and accept charge from PP sheet surface. (c) As condensed droplets fall off, the charge is carried with the droplet and overall PP sheet is left neutral.[40]

For future investigations, the effect of the present sanitization condition on other mask components such as ear loops and nose clips should be characterized. In addition, much of the surface potential of electret-based filters can be lost during normal usage; in consideration of this, an additional re-charging stage can be implemented, such as exposure to corona discharge.

Although filtration efficiency of sub-300 nm particles was inferred by surface potential, proper filtration efficiency tests on commercial facemasks (surgical, N95 grade, and dense cartridge based) is recommended. In addition, the current sanitization condition can be applied to disinfect a multitude of surfaces. Although O_3 generation may prove cumbersome, backpack or handheld nebulization of H_2O_2 is currently utilized to disinfect high-touch surfaces. A simple modification of the process by incorporating a flash lamp can enhance the biocidal effect of H_2O_2; this modification will also extend existing supplies of aqueous H_2O_2 as the synergistic regime achieves potent disinfection at diluted H_2O_2 concentrations.

Ideally, the present study should have incorporated viral samples, especially the SARS-CoV-2 virus. However, due to regulatory and time limitations, commercially available *G. stearothermophilus* was utilized as a model organism. These spore discs have been previously utilized to test the biocidal efficacy of commercial sanitization equipment as well as other vaporous H_2O_2 processes. In addition, IPL exposure requires surfaces free from obstruction. The disposable masks will have to be unfolded and properly oriented to achieve optimal IPL surface exposure. Although these limitations of IPL exposure affect scalability, the flashing regime only takes a few seconds. In comparison, the Battelle Critical Care Decontamination System™ (CCDS™) is a proprietary N95 mask decontamination service; this process was quoted to achieve decontamination of 80 000 masks per day using VHP exposure for 2.5 h[44] It is important to note that the proprietary CCDS™ VHP process parameters were not disclosed. However, if assuming the methodology is similar to the Battelle report on VHP decontamination for N95 masks (where *G. stearothermophilus* was also utilized), comparisons can be made.[20] The optimized VHP process in the report quotes a 20 min gassing phase at 2 g min^{-1} H_2O_2 followed by 150 min of dwell time at 0.5 g min^{-1} H_2O_2. Thus, the optimized synergistic sanitization method presents a potential 68.6% reduction in H_2O_2 consumption relative to the Battelle CCDS™ process. In addition, the novel synergistic sanitization regime achieved decontamination at 30 min of fumigation followed by a few seconds of IPL irradiation. The novel synergistic also did not require dehumidification prior to sanitization nor post sanitization drying.

5. Conclusions

In the present study, a novel sanitization method was able to increase the sanitization potency of VHP treatment on

Open Access Article. Published on 07 July 2021. Downloaded on 12/5/2025 4:10:48 AM.
This article is licensed under a Creative Commons Attribution-NonCommercial 3.0 Unported Licence.

polymeric-based filters such as PP. After exposure to the optimized sanitization regime, little to no change in important performance metrics was observed on PP filter sheets including: saline droplet filtration efficiency, surface potential, tensile strength, and biosafety. By introducing 3 g h^{-1} O_3 flow during VHP fumigation followed by 10 IPL flashes (on both disc faces), complete inactivation of *G. stearothermophilus* spore discs was achieved. Initial tests showed nebulized 3% H_2O_2 aqueous solution was unable to sanitize the spore discs; however, introduction of O_3 and IPL synergistic elements achieved inactivation of indicator spores at aqueous H_2O_2 feed concentrations as low as 0.03%. The increased sanitization strength was attributed to: introduction of biocidal species H_2O_3; improved H_2O_2 biocidal performance *via* the photo-Fenton reaction; and the increased population of previously present biocidal ROS *via* advanced oxidation mechanisms. After exposure to the optimized regime, no severe loss of 300 nm to 3000 nm net neutral saline water aerosol droplets was observed. A small 5% loss in magnitude of surface potential was observed (preserving surface potential is critical for the capture of sub-300 nm particles). Triplicate tensile tests revealed slight embrittlement as yield strain decreased from 3.97% (yield stress: 1.70 ± 0.25 MPa) to 3.03% (yield stress: 1.75 ± 0.17 MPa) before and after treatment, respectively. In addition, ATR FT-IR characterization revealed near identical spectra before and after sanitization indicating biosafety and no significant structural changes. In comparison to the commercially available Bioquell BQ-50, the optimized regime required 67.8% less H_2O_2 to sanitize the indicator spores. The potent synergistic effect provides a pathway to sanitize and re-use polymeric based filters with minimal H_2O_2 consumption. With no active temperature or humidity control requirements, the optimized sanitization regime has competitive potential for scalability.

Abbreviations

VHP	Vaporous hydrogen peroxide
H_2O_2	Hydrogen peroxide
O_3	Ozone
IPL	Intense pulsed light
PP	Polypropylene
COVID-19	Coronavirus disease 2019
SARS-CoV-2	Severe acute respiratory syndrome coronavirus 2
PPE	Personal protective equipment
UGI	Ultraviolet germicidal irradiation
G. stearothermophilus	*Geobacillus stearothermophilus*
FFR	Filtering facepiece respirator
IPA	Isopropyl alcohol
MPPS	Most penetrating particle size
ROS	Reactive oxygen species
TSB	Tryptic soy broth
ATR FT-IR	Attenuated total reflection fourier transform infrared spectroscopy

Author contributions

All authors contributed to the writing of the paper. Authors Robin Jeong and Hitendra Kumar optimized the sanitization regime and performed mechanical characterizations; in addition, these authors explored the underlying mechanisms and reported them in the present paper. Author Steven Jones performed provided consultation regarding indicator spore choice as well as incubation methodology. Dr Jones performed incubation of the spore discs after sanitization in the Zymetrix facilities at University of Calgary. Author Allen Sandwell constructed and developed the methodology of the sanitization chamber and filtration efficiency setups. Authors Keekyoung Kim and Simon S. Park first conceptualized the project and provided continued supervision and writing editing/review.

Conflicts of interest

The authors have no conflicts of interest to declare.

Acknowledgements

We would like to acknowledge the Natural Sciences and Engineering Research Council (NSERC) of Canada, Alberta Innovates Campus Alberta Small Business Engagement and Trium Environmental Inc. for supporting this research. We would like to thank Tyler Horton and Leif Blake who assisted in the experiments.

References

1 *WHO COVID-19 Weekly Epidemiological Update*, https://www.who.int/publications/m/item/weekly-epidemiological-update-on-covid-19-4-may-2021, accessed May, 4, 2021.
2 O. O. Fadare and E. D. Okoffo, *Sci. Total Environ.*, 2020, **737**, 140279.
3 A. Konda, A. Prakash, G. A. Moss, M. Schmoldt, G. D. Grant and S. Guha, *ACS Nano*, 2020, **14**, 6339–6347.
4 M. C. Celina, E. Martinez, M. A. Omana, A. Sanchez, D. Wiemann, M. Tezak and T. R. Dargaville, *Polym. Degrad. Stab.*, 2020, **179**, 109251.
5 H. P. Kim, M. S. Jo, C. H. Kim, J. S. Choi and I. J. Yu, *NanoImpact*, 2020, **19**, 100231.
6 Q. Ou, C. Pei, S. Chan Kim, E. Abell and D. Y. H. Pui, *J. Aerosol Sci.*, 2020, **150**, 105609.
7 D. Wang, B.-C. Sun, J.-X. Wang, Y.-Y. Zhou, Z.-W. Chen, Y. Fang, W.-H. Yue, S.-M. Liu, K.-Y. Liu, X.-F. Zeng, G.-W. Chu and J.-F. Chen, *Engineering*, 2020, **6**, 1115–1121.
8 D. Zoutman, M. Shannon and A. Mandel, *Am. J. Infect. Control*, 2011, **39**, 873–879.
9 W. W. F. Leung and Q. Sun, *Sep. Purif. Technol.*, 2020, **250**, 116886.
10 A. Kumar, S. B. Kasloff, A. Leung, T. Cutts, J. E. Strong, K. Hills, G. Vazquez-Grande, B. Rush, S. Lother, R. Zarychanski and J. Krishnan, *medRxiv*, 2020, DOI: 10.1101/2020.04.05.20049346.

© 2021 The Author(s). Published by the Royal Society of Chemistry

Open Access Article. Published on 07 July 2021. Downloaded on 12/5/2025 4:10:48 AM.
This article is licensed under a Creative Commons Attribution-NonCommercial 3.0 Unported Licence.

11 L. Pirker, A. P. Krajnc, J. Malec, V. Radulović, A. Gradišek, A. Jelen, M. Remškar, I. B. Mekjavić, J. Kovač, M. Mozetič and L. Snoj, *J. Membr. Sci.*, 2021, **619**, 118756.
12 D. Kanakaraju, B. D. Glass and M. Oelgemöller, *J. Environ. Manage.*, 2018, **219**, 189–207.
13 M. Y. Alkawareek, A. Bahlool, S. R. Abulateefeh and A. M. Alkilany, *PLoS One*, 2019, **14**, e0220575.
14 H. Hayrapetyan, L. Nederhoff, M. Vollebregt, H. Mastwijk and M. Nierop Groot, *Int. J. Food Microbiol.*, 2020, **316**, 108418.
15 L. E. Murdoch, L. Bailey, E. Banham, F. Watson, N. M. T. Adams and J. Chewins, *Lett. Appl. Microbiol.*, 2016, **63**, 178–182.
16 A. Pandey, K. Dhakar, P. Sati, A. Sharma, B. Kumar and L. M. S. Palni, *Proc. Natl. Acad. Sci., India, Sect. B*, 2014, **84**, 349–356.
17 C. Yim, A. Sandwell and S. S. Park, *ACS Appl. Mater. Interfaces*, 2016, **8**, 22369–22373.
18 M. Lindblad, E. Tano, C. Lindahl and F. Huss, *Burns*, 2020, **46**, 842–849.
19 P. P. Tsai, H. Schreuder-Gibson and P. Gibson, *J. Electrost.*, 2002, **54**, 333–341.
20 Battelle, *Final Report for Bioquell HPV Decontamination for Reuse of N95 Respirators*, FDA, 2016.
21 M. S. Bergman, Z. Zhuang, D. Hanson, B. K. Heimbuch, M. J. McDonald, A. J. Palmiero, R. E. Shaffer, D. Harnish, M. Husband and J. D. Wander, *J. Occup. Environ. Hyg.*, 2014, **11**, 117–125.
22 S. Radl, S. Ortner, R. Sungkorn and J. G. Khinast, *Journal of Pharmaceutical Innovation*, 2009, **4**, 51–62.
23 T. Pottage, C. Richardson, S. Parks, J. T. Walker and A. M. Bennett, *Journal of Hospital Infection*, 2010, **74**, 55–61.
24 P. Gijsman, M. Kroon and M. van Oorschot, *Polym. Degrad. Stab.*, 1996, **51**, 3–13.
25 M. J. Walzak, S. Flynn, R. Foerch, J. M. Hill, E. Karbashewski, A. Lin and M. Strobel, *J. Adhes. Sci. Technol.*, 1995, **9**, 1229–1248.
26 Y. Wang, J. Kim, K.-H. Choo, Y.-S. Lee and J. Lee, *J. Membr. Sci.*, 2000, **169**, 269–276.
27 R. Morent, N. De Geyter, C. Leys, L. Gengembre and E. Payen, *Surf. Interface Anal.*, 2008, **40**, 597–600.
28 V. E. Caudill and G. W. Halek, *J. Plast. Film Sheeting*, 1992, **8**, 140–154.
29 E. Linley, S. P. Denyer, G. McDonnell, C. Simons and J.-Y. Maillard, *J. Antimicrob. Chemother.*, 2012, **67**, 1589–1596.
30 G. Brandi, L. Salvaggio, F. Cattabeni and O. Cantoni, *Environ. Mol. Mutagen.*, 1991, **18**, 22–27.
31 P. Kumkrong, L. Scoles, Y. Brunet, S. Baker, P. H. J. Mercier and D. Poirier, *J. Hosp. Infect.*, 2021, **111**, 117–124.
32 E. P. Manning, M. D. Stephens, S. Dufresne, B. Silver, P. Gerbarg, Z. Gerbarg, C. S. Dela Cruz and L. Sharma, *BMJ Open Respiratory Research*, 2021, **8**, e000781.
33 M.-E. Dubuis, N. Dumont-Leblond, C. Laliberté, M. Veillette, N. Turgeon, J. Jean and C. Duchaine, *PLoS One*, 2020, **15**, e0231164.
34 A. J. Brodowska, A. Nowak and K. Śmigielski, *Crit. Rev. Food Sci. Nutr.*, 2018, **58**, 2176–2201.
35 T. W. Ng, T. An, G. Li, W. K. Ho, H. Y. Yip, H. Zhao and P. K. Wong, *J. Photochem. Photobiol., B*, 2015, **149**, 164–171.
36 G. Merényi, J. Lind, S. Naumov and C. v. Sonntag, *Environmental Science & Technology*, 2010, **44**, 3505–3507.
37 X. Xu and W. A. Goddard, *Proc. Natl. Acad. Sci. U. S. A.*, 2002, **99**, 15308.
38 N. H. Ince, *Water Environ. Res.*, 1998, **70**, 1161–1169.
39 Y. Wen, Z. Yuan, J. Qu, C. Wang and A. Wang, *ACS Sustainable Chem. Eng.*, 2020, **8**, 2688–2697.
40 T. Ohmi, S. Sudoh and H. Mishima, *IEEE Transactions on Semiconductor Manufacturing*, 1994, **7**, 440–446.
41 T. J. Swanson, Z. Jamal and J. Chapman, *Ozone Toxicity*, StatPearls Publishing, Treasure Island (FL), 2020.
42 A. D. Fryer, D. B. Jacoby and S. A. Wicher, *Res. Rep.–Health Eff. Inst.*, 2017, 1–41.
43 P. A. Kenney, B. K. Chan, K. E. Kortright, M. Cintron, M. Russi, J. Epright, L. Lee, T. J. Balcezak, N. L. Havill and R. A. Martinello, *Infect. Control Hosp. Epidemiol.*, 2021, 1–3.
44 *Battelle CCDS Critical Care Decontamination System™ Being Deployed to Meet Urgent Need for Personal Protective Equipment for Nation's Healthcare Workforce*, https://www.battelle.org/newsroom/press-releases/press-releases-detail/battelle-ccds-critical-care-decontamination-system-being-deployed-to-meet-urgent-need-for-personal-protective-equipment-for-nation-s-healthcare-workforce, accessed May, 6, 2021.